Detrended fluctuation analysis of seismicity and order parameter fluctuations before the M7.1 Ridgecrest earthquake

Skordas, E. S., Christopoulos, S. & Sarlis, N. V.

Original citation & hyperlink:
Skordas, ES, Christopoulos, S & Sarlis, NV 2020, 'Detrended fluctuation analysis of seismicity and order parameter fluctuations before the M7.1 Ridgecrest earthquake', Natural Hazards, vol. 100, no. 2, pp. 697-711.
https://doi.org/10.1007/s11069-019-03834-7

DOI 10.1007/s11069-019-03834-7
ISSN 0921-030X
ESSN 1573-0840

Publisher: Springer

The final publication is available at Springer via http://dx.doi.org/10.1007/s11069-019-03834-7

Detrended Fluctuation Analysis of seismicity and Order Parameter Fluctuations before the M7.1 Ridgecrest earthquake

Efthimios S. Skordas · Stavros-Richard G. Christopoulos · Nicholas V. Sarlis

Abstract Detrended fluctuation analysis (DFA) has been recently applied for the investigation of temporal correlations between the earthquake magnitudes before major earthquakes. Here we employ DFA together with natural time analysis in order to identify precursory phenomena to the M7.1 Ridgecrest earthquake on July 6, 2019. The analysis reveals that a minimum of the variability of the order parameter of seismicity in natural time is observed almost a month before the occurrence of this earthquake. This minimum was observed when DFA indicated the development of the presence of long range correlations which turned to an almost random behavior before the strong earthquake. Upon starting the study of seismicity in natural time from the minimization of the variability on June 5, 2019, we conclude that criticality has been reached at 22:41 UTC on July 2, 2019, almost 3 days before the earthquake occurrence. The application of an algorithm based on the coherent noise model would have led to a warning 3 minutes before the occurrence of the M7.1 Ridgecrest earthquake.

Keywords Detrended Fluctuation Analysis · earthquakes · natural time analysis · order parameter of seismicity · coherent noise model

1 Introduction

Earthquakes (EQs) are complex phenomena(Rundle et al., 2000; Kanamori and Brodsky, 2001) mainly related with the tectonic structure of the Earth(Bird, 2003).

E.S. Skordas
Section of Solid State Physics and Solid Earth Physics Institute, Department of Physics, National and Kapodistrian University of Athens, Panepistimiopolis, Zografos 157 84, Greece
Tel.: +30-210-7276735, Fax: +30-210-9601721, E-mail: eskordas@phys.uoa.gr

S.-R.G. Christopoulos
Faculty of Engineering, Environment and Computing, Coventry University, Priory Street, Coventry, CV1 5FB, United Kingdom
Tel.: +44-747-0036853, E-mail: ac0966@coventry.ac.uk

N.V. Sarlis
Section of Solid State Physics and Solid Earth Physics Institute, Department of Physics, National and Kapodistrian University of Athens, Panepistimiopolis, Zografos 157 84, Greece
Tel.: +30-210-7276736, Fax: +30-210-9601721, E-mail: nsarlis@phys.uoa.gr

They have been the subject of a multitude of studies (e.g., see Lennartz et al., 2008; Huang, 2008; Lippiello et al., 2008; Telesca and Lovallo, 2009; Huang, 2011; Lennartz et al., 2011; Huang and Ding, 2012; Rundle et al., 2012, 2016; Luginbuhl et al., 2018; Rundle et al., 2019) that focus on their correlations in time, space and magnitude (M) and have been found to obey a variety of scaling laws (e.g., see Chapter 6 Varotsos et al., 2011c) including the Gutenberg-Richter law(Gutenberg and Richter, 1956) (that effectively states that the probability to observe an EQ of energy E is a power law, $P(E) \propto E^{-\delta}$, where $\delta \approx 1.66$) the Omori-Utsu law (Utsu et al., 1995) (that roughly states that the number of aftershocks versus the conventional time elapsed from the mainshock decays as a power law), etc. Turcotte (1997) proposed that these EQ scaling laws indicate the proximity of the system to a critical point and nowadays such an perspective is widely accepted (e.g. see Varotsos et al., 2001; Carlson et al., 1994; Holliday et al., 2006; Varotsos et al., 2011c).

The existence of long-range correlations between the elements of a (zero-mean) time-series, $\tilde{x}_i$, leads to an autocorrelation function:

$$C(s) = \frac{\langle \tilde{x}_i \tilde{x}_{i+s} \rangle}{\langle \tilde{x}_i^2 \rangle} = \frac{N}{(N-s)} \frac{\sum_{i=1}^{N-s} \tilde{x}_i \tilde{x}_{i+s}}{\sum_{i=1}^{N} \tilde{x}_i^2} \tag{1}$$

that instead of decaying exponentially, cf. $C(s) \propto \exp(-s/\tau)$), decreases as a power law

$$C(s) \propto s^{-\gamma} \tag{2}$$

with an exponent(Kantelhardt et al., 2001) in the range $0 < \gamma < 1$. Probably the most well established method for estimating long-range correlations in time-series is the Detrended Fluctuation Analysis (DFA) (Peng et al., 1994, 1995a) which employs a random walker approach (see Section 2 below) in order to determine a scaling exponent labeled a (see pp.24-26 of Varotsos et al., 2011c). If $a \approx 0.5$ a random white noise behavior is expected, while for $0.5 < a < 1$, the scaling exponent a is interconnected with the correlation exponent γ through the relation $\gamma = 2 - 2a$. One of the main advantages of DFA, is that it has been developed (Peng et al., 1993, 1994; Buldyrev et al., 1995; Taqqu et al., 1995; Talkner and Weber, 2000; Hu et al., 2001; Chen et al., 2002, 2005; Xu et al., 2005) for the quantification of long range correlations in non-stationary signals. Thus, it has been applied to a multitude of fields including DNA(Carpena et al., 2002), human motor activity(Hu et al., 2004) and gait(Ashkenazy et al., 2002), cardiac dynamics(Ivanov et al., 1998), meteorology(Ivanova and Ausloos, 1999), climate temperature fluctuations(Koscielny-Bunde et al., 1998), solar incident flux (Varotsos et al., 2015a), etc. As suggested by Talkner and Weber (2000) and Xu et al. (2005), common approaches like power spectrum and autocorrelation analysis(Stratonovich, 1981) are not suitable for non-stationary signals. Seismicity, being another example of non-stationary signal due to the existence of aftershocks, has been also studied by DFA to which we now turn.

Telesca et al. (2003) applied DFA to the seismicity of Italy and confirmed the presence of long-range behavior in the temporal distribution for the both the original and the aftershock-depleted catalogues. Lennartz et al. (2008) studied the regimes of stationary seismic activity in Northern and Southern California by DFA and found that long-range correlations exist in the time-series of EQ magnitudes for M$\geq$ 2 with $a = 0.59 \pm 0.05$. Later, a DFA study (see Fig. 3 of Sarlis et al.,

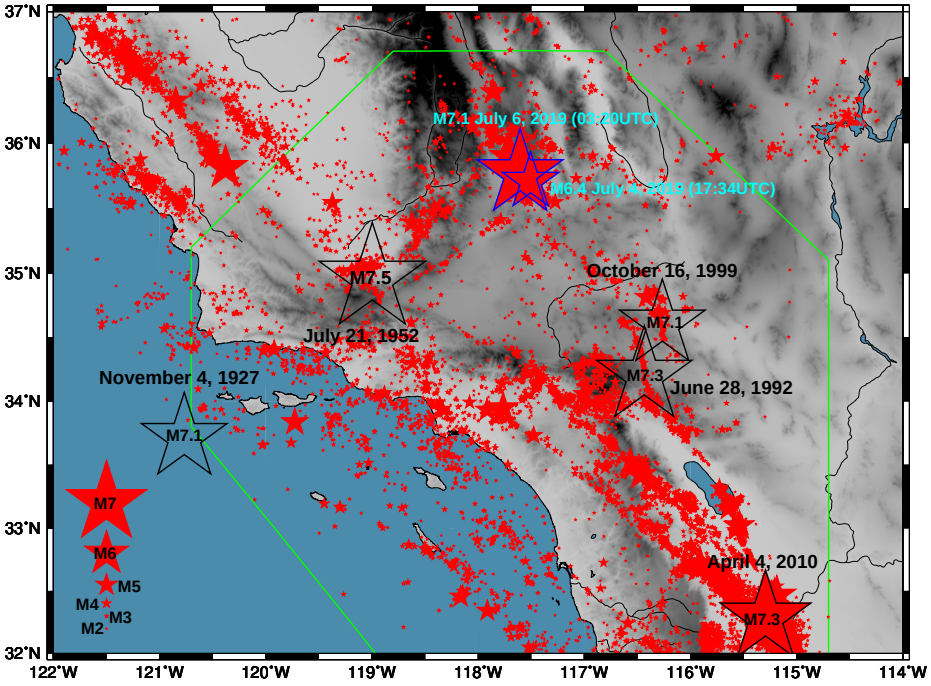

Fig. 1 (color online) Map depicting the EQs with mangitude M≥2.0 reported by the Southern California Earthquake Center (SCEC) since 1 January 2004 (red stars). In addition to the 2010 El Mayor-Cucapah M7.3 EQ, the strongest EQs of the last 100 years (1927 Lompoc M7.1, 1952 Kern County M7.5, 1992 Landers M7.3 and the 1999 Hector Mine M7.1 EQ) are also depicted by black stars. The two recent Ridgecrest EQs are depicted with blue stars. The green line delimits the geographic polygon shown in Fig.1 of Hauksson et al. (2012) that covers the Southern California Seismic Network reporting area for local events.

2010b) of the EQ magnitude time-series in Southern California has shown that the exponent a exhibits values lower than those found in the aforementioned regimes of stationary seismicity before strong EQs like the 1992 M7.3 Landers and the 1999 M7.1 Hector Mine EQs (their epicenters are shown in Fig.1). It is noteworthy that the long-range correlations found in the EQ magnitude time-series are neccessary (Sarlis et al., 2010a) for the successful reproduction of the properties found when analyzing the Japanese and the Southern Californian seismicity in natural time.

Natural time analysis (Varotsos et al., 2001, 2002a,b, 2011c,b; Sarlis, 2017; Sarlis et al., 2018b) is a modern method for the analysis of complex systems that enables the introduction (Varotsos et al., 2005) of an order parameter for seismicity within the aforementioned view that EQs are critical phenomena. The study (Sarlis et al., 2013; Varotsos et al., 2013; Sarlis et al., 2015; Varotsos et al., 2017b; Sarlis et al., 2018a, 2019a) of the fluctuations of this order parameter has shown that it exhibits characteristic minima before strong EQs which appear simultaneously (Varotsos et al., 2013) with the initiation of the emission of Seismic Electric Signals (SES) activities (Varotsos and Lazaridou, 1991; Varotsos et al., 1993; Varotsos, 2005). The latter are precursory low frequency (≤ 0.1Hz) electric signals observed a few weeks to $5\frac{1}{2}$ months before major EQs (Varotsos et al., 2011c) that allow (Sarlis et al., 2018c) the determination of the epicenter location and occurrence

time of an impending strong EQ. Their generation can be understood on the basis of a thermodynamical model(Varotsos et al., 2019).

The combined study of the order parameter fluctuations of seismicity with the DFA of EQ magnitude time-series in California, Japan and Mexico, has revealed (Varotsos et al., 2012, 2014; Sarlis et al., 2019b) that the temporal correlations between EQ magnitudes exhibit a characteristic change from long-range to random after the minimization of the order parameter fluctuations and before the strong EQ occurrence. In view of the fact, that these precursory phenomena may be used for the anticipation of a strong EQ it is the scope of the present paper to investigate what happened before the recent 2019 Ridgecrest M7.1 EQ.

The paper is organized as follows: Section 2 presents the theoretical background of DFA (Subsect. 2.1) and natural time analysis (Subsect. 2.2) while Sect. 3 decribes the data analyzed. The results follow in Sect. 4 and their discussion in Sect. 5. Finally, the conclusions are summarized in Sect. 6.

2 Theoretical Background

2.1 Detrended Fluctuation Analysis

As already mentioned, DFA is a robust method suitable for detecting long-range power law correlations within non-stationary signals. As we will see below, the major advantage of DFA is the systematic elimination of polynomial trends of different orders(Bunde et al., 2000; Kantelhardt et al., 2001; Hu et al., 2001; Bashan et al., 2008). DFA is based on random walk theory and its brief description is as follows: Once we have a time series x_i, $i = 1, 2, ..., N$, we first calculate the zero-mean time-series $\tilde{x}_i \equiv x_i - \overline{x}$ by subtracting the mean $\overline{x} = \sum_{i=1}^{N} x_i/N$, and construct the profile $y(n) = \sum_{i=1}^{n} \tilde{x}_i$. The profile can be considered as the position of an one-dimensional random walker after n steps. Then, $y(n)$ is divided into $N_s \equiv [N/s]$ non overlapping segments of equal number of steps ("scale") s and a polynomial trend $y_s^{(l)}(n)$ within each segment is determined by least-squares fitting (cf. $y_s^{(l)}(n)$ stands for the concatenated polynomials of order l which are calculated separately for each of the segments). The degree of the polynomial can be varied in order to eliminate linear ($l = 1$), quadratic ($l = 2$), or higher order trends (Bunde et al., 2000) of the profile function (in our study here we used $l = 1$). Finally, the fluctuation function $F(s)$ on scale s is estimated by means of the detrended profile function $\tilde{y}_s(n) \equiv y(n) - y_s^{(l)}(n)$ through the formula

$$F(s) = \sqrt{\frac{1}{N}\sum_{n=1}^{N}[\tilde{y}_s(n)]^2}. \tag{3}$$

$F(s)$ can be considered as the trend-eliminated root mean square displacement of the random walker mentioned above. A power law relation between $F(s)$ and s, i.e.,

$$F(s) \sim s^a \tag{4}$$

indicates the presence of scale-invariant (fractal) behavior embedded in the fluctuations of the signal. The fluctuations can be characterized by the scaling exponent

a: If $a = 0.5$, there are no correlations in the data and the signal is uncorrelated (white) noise; the case $a < 0.5$ corresponds to anti-correlations, meaning that large values are most likely to be followed by small values and vice versa. If $a > 0.5$, there are long range correlations, which are stronger(Bashan et al., 2008) for higher a. The grey circles in Figs. 2(c) and 3 depict the values obtained for the DFA exponent a_{300} when analysing the EQ magnitude in consecutive segments of the EQ catalog comprising 300 EQs (cf. since we employed the computer code `dfa.c`, originally from Peng et al. 1995b, which is publicly available from Physionet, see Goldberger et al. 2000, the scale range used to estimate this DFA exponent was 4 to 70). The selection of this crucial scale (Varotsos et al., 2011a) has been made on similar grounds as the ones explained by Varotsos et al. (2014), see also Sect. 4.

2.2 Natural Time Analysis

In a time series comprising N EQs, the natural time $\chi_k \equiv k/N$ and serves as an index for the occurrence of the k-th event. This index together with the energy Q_k released during the k-th EQ of magnitude M_k, i.e., the pair (χ_k, Q_k), is studied in natural time analysis. One computes alternatively the pair (χ_k, p_k), where $p_k = Q_k / \sum_{n=1}^{N} Q_n$ denotes the normalized energy released during the k-th EQ. Q_k, and hence p_k, is estimated (e.g. see Tanaka et al., 2004) through the relation (Kanamori, 1978)

$$Q_k \propto 10^{1.5\mathrm{M}_k}. \tag{5}$$

The variance of χ weighted for p_k, labeled κ_1, is given by (Varotsos et al., 2001, 2003a,b, 2011c, 2005, 2011a)

$$\kappa_1 = \sum_{k=1}^{N} p_k (\chi_k)^2 - \left(\sum_{k=1}^{N} p_k \chi_k \right)^2. \tag{6}$$

Varotsos et al. (2005) have explained that the variance κ_1 given by Eq. (6) can be considered as an order parameter for seismicity since its value changes abruptly when a mainshock (the new phase) occurs, and in addition the statistical properties of its fluctuations resemble those in other non-equilibrium and equilibrium critical systems(see also Sarlis et al., 2011). It has been found (Varotsos et al., 2001, 2002a, 2011c,b) that when the variance κ_1 converges to 0.070 the evolving complex dynamical system under study enters the critical stage (for a recent example concerning EQs see Varotsos et al., 2017a).

Upon considering a moving natural time window comprising W consecutive events sliding, event by event, through an EQ catalog the computed κ_1 values enable the calculation of their average value $\mu(\kappa_1)$ and their standard deviation $\sigma(\kappa_1)$ and the hence a quantification of the fluctuations of the order parameter of seismicity. To this purpose, we determine (Sarlis et al., 2010b; Varotsos et al., 2011c,a; Sarlis et al., 2013, 2015) the variability β of κ_1, i.e., the quantity β_W

$$\beta_W = \frac{\sigma(\kappa_1)}{\mu(\kappa_1)}. \tag{7}$$

that corresponds to this natural time window of length W. The time evolution of β_W is then pursued by ascribing to it the conventional time of occurrence

of the next EQ in the catalog as shown in Figs.2 and 3. As mentioned in the Introduction, Varotsos et al. (2013) showed that the seismicity order parameter fluctuations exhibit a variability minimum β_{min} upon the initiation of a series of precursory SES, as for example the ones recorded by Uyeda et al. (2002, 2009) in Japan. In a similar fashion, the minimum β_{min} of the fluctuations of the order parameter of seismicity before the M9 Tohoku EQ that occurred on 11 March 2011 (which was the deepest minimum ever observed in Japan during the period 1984-2011 investigated) was observed (Sarlis et al., 2013) on 5 January 2011 almost simultaneously with the initiation of anomalous magnetic field variations on the vertical component accompanying an SES activity(a mechanism that may lead to such a phenomenon can be found in Sarlis and Varotsos, 2002). Actually, Xu et al. (2013); Han et al. (2015, 2016) reported that during the period 4 to 14 January 2011 at two measuring sites (Esashi and Mizusawa) lying at epicentral distances of around 130km such anomalous magnetic field variations have been observed.

3 Data Analyzed

The EQ catalog of the Southern California Earthquake Center (SCEC), available at `http://service.scedc.caltech.edu/ftp/catalogs/SCEC_DC/`, has been used. Our study was focused on the period January 1, 2004, until the Ridgecrest EQ occurrence on July 6, 2019 (cf. for an earlier period the seismicity in California has been studied in natural time by Varotsos et al., 2011a, 2012). The epicenters of all EQs with magnitude larger than or equal to the threshold $\mathrm{M_{thres}} = 2.0$ are shown by the red stars in Fig.1. Following our previous work (Christopoulos and Sarlis, 2017), we focused in the analysis of seismicity within the geographic polygon shown in Fig.1 of Hauksson et al. (2012) that covers the Southern California Seismic Network reporting area for local events that is depicted by the green line in Fig.1. The magnitude of EQs within this area can be read in the right-hand scale of Figs.2 and 3. Such an analysis results in 28,367 EQs in the concerned period (January 1, 2004, until the Ridgecrest EQ) of roughly 13.5 years or equivalently to a monthly rate of 175 EQs/mo.

4 Results

Figure 2 depicts the time evolution of the variability β_W of the order parameter of seismicity for W =200, 250, 300, 350, 400, 450, and 500 together with that of the DFA exponent a_{300} (see the grey circles in Fig.2(c)) estimated when using a moving window of 300 events. The selection of the W values is such that they correspond to a time period of a few months (cf. the monthly rate is 175 EQs/mo) so that they compare favourably with the SES lead time as suggested by (Varotsos et al., 2011a). The colored horizontal lines correspond to the minimum values of β_W that have been observed almost one month before the 2019 Ridgecrest EQ. The behavior a few months before the latter EQ in expanded time scale can be seen in Fig.3 which presents both the aforementioned β_W and the DFA exponent a. A closer look of Fig.2 reveals that for W =300, 350, 400, and 450 the minima are observed on June 5, 2019, see Fig.3(c), being the deepest ones for the whole study period (cf. for W =350 the minimum lasts from June 2 up to June 5, 2019).

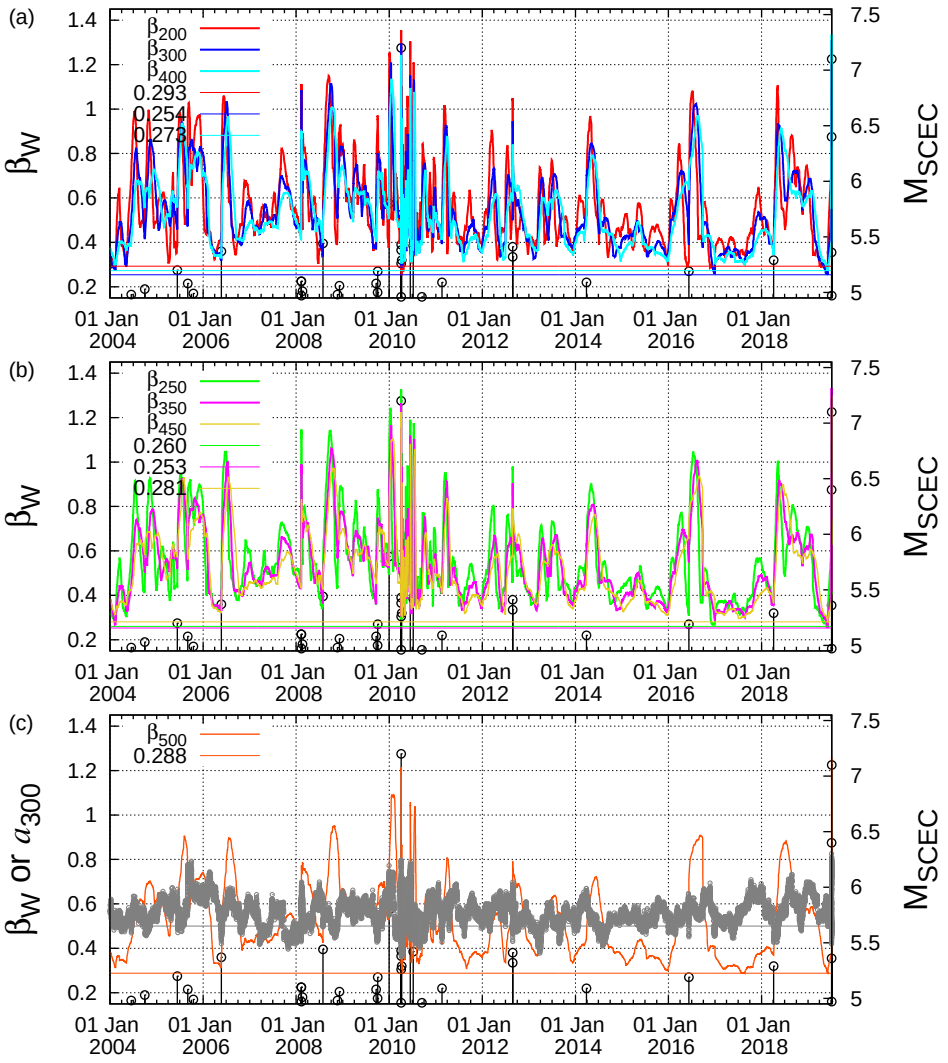

Fig. 2 (color online) The variabilities β_W for W=200 (red), 250 (green), 300 (blue), 350 (magenta), 400 (cyan), 450 (gold), and 500 (orange) together with the DFA exponent a_{300} (grey circles) versus the conventional time since January 1, 2004 until the occurrence M7.1 Ridgecrest EQ on July 6, 2019. The vertical bars ending at circles correspond to the EQ magnitude reported by SCEC and are read in the right scale. The horizontal lines correspond to the β_W minima that have been observed during he period May 29, 2019 until June 5, 2019 and have been drawn as a guide to the eye.

This fact together with the observed behavior of the DFA exponent a_{300} will be discussed in the next Section.

As mentioned in the previous Sections, the observation of β_{min} is almost simultaneous with the initiation of an SES activity signaling that a study of the seismicity in natural time in the area prone to suffer the strong EQ may lead to an estimation of the occurrence time of the impending EQ (Varotsos et al., 2008;

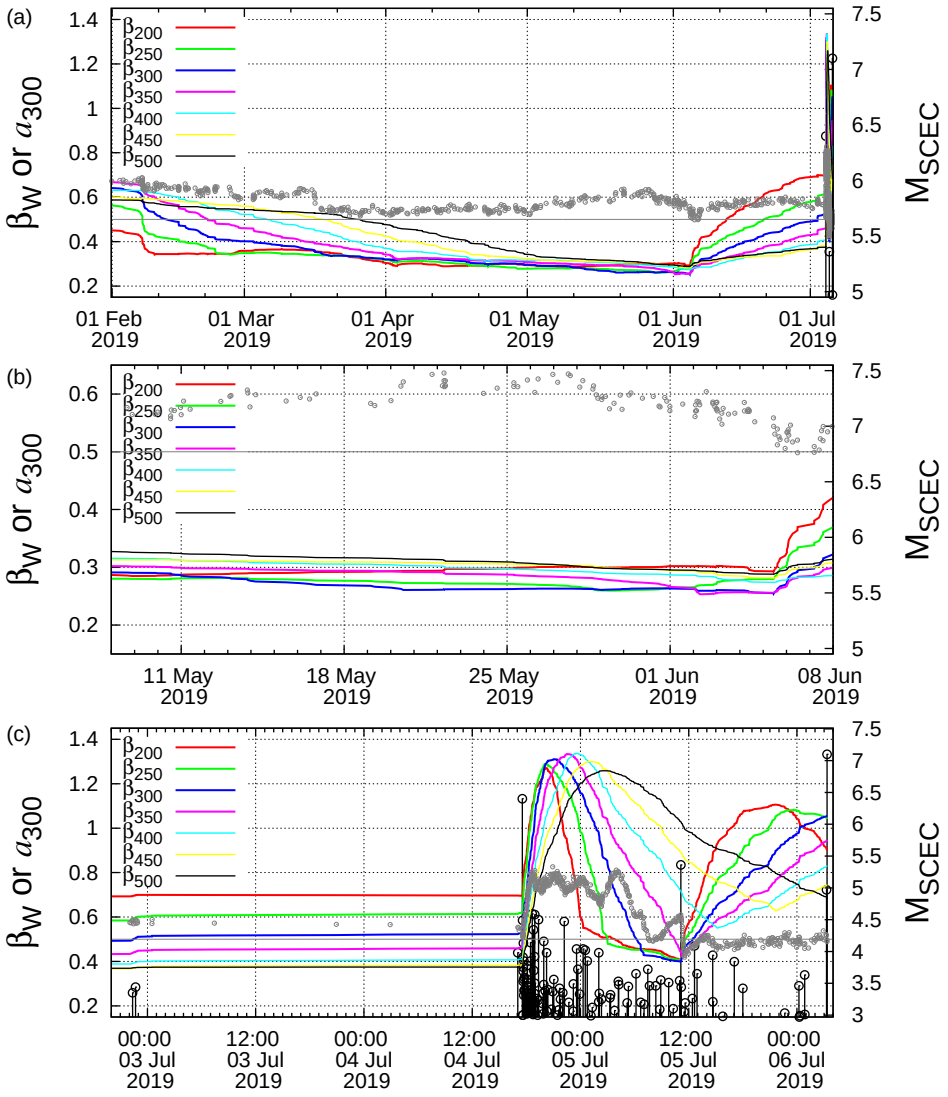

Fig. 3 (color online) Excerpts of Fig. 2 for the time periods: (a) February 1, 2019 until the occurrence M7.1 Ridgecrest EQ, (b) May 8 to June 8, 2019, (c) July 2 at 20:00 UTC until the occurrence M7.1 Ridgecrest EQ at 03:20 UTC on July 6, 2019.

Sarlis et al., 2008; Varotsos et al., 2010, 2011c; Sarlis, 2013; Skordas and Sarlis, 2014; Varotsos et al., 2015b, 2017a; Sarlis and Skordas, 2018; Sarlis et al., 2019a). Once an SES activity has been recorded at a measuring station, the SES properties (Varotsos, 2005; Varotsos et al., 2011c; Sarlis et al., 2018c) allow the determination of the area candidate to suffer the EQ by means of the so-called 'selecitivity' map (Varotsos and Lazaridou, 1991; Varotsos et al., 1993) that includes all the seismogenic areas that gave rise to SES at a given measuring station in the past. Since in our case, however, SES information is not available we have to follow the

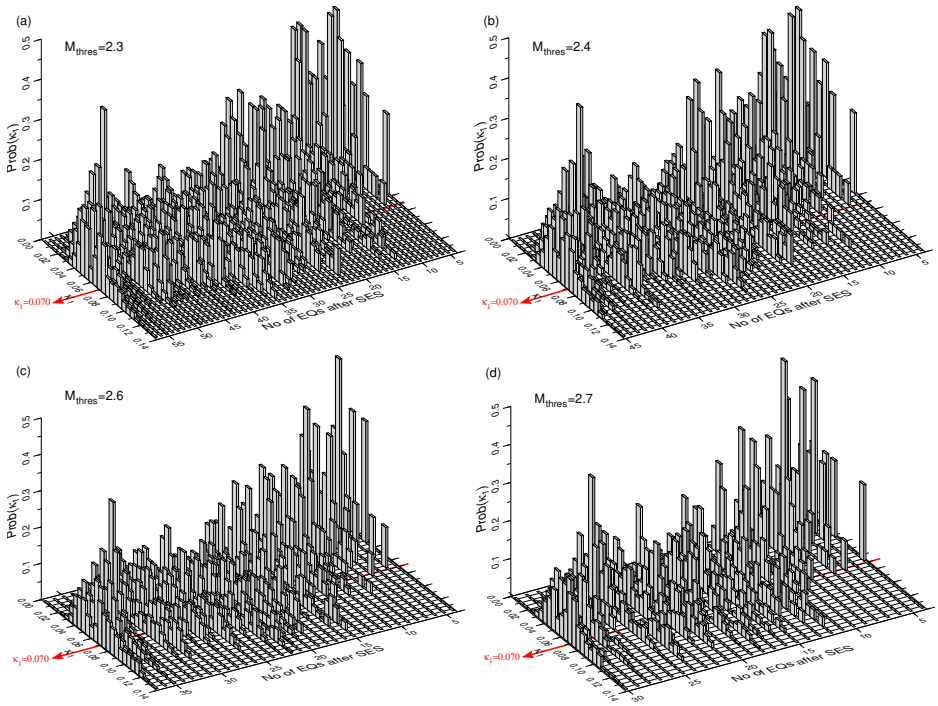

Fig. 4 (color online) The probability distribution Prob(κ_1) of κ_1 versus κ_1 as it results after the occurrence of each small EQ within the area delimited by the green polygon in Fig.1 for the magnitude thresholds: (a)$M_{\rm thres}$=2.3, (b)$M_{\rm thres}$=2.4, (c)$M_{\rm thres}$=2.6, and (d)$M_{\rm thres}$=2.7 after the minimization of the variability of the order parameter of seismicity on June 5, 2019. The last event considered is the M3.4 EQ at 22:41 UTC on July 2, 2019 at 35.050^{o}N 118.936^{o}W.

method suggested by Sarlis et al. (2008) for the estimation of the occurrence time of the impending strong EQ by analyzing in natural time all the small EQs of magnitude greater than or equal to $M_{\rm thres}$ that occurred after the aforementioned minimization of the fluctuations of the order parameter of seismicity on June 5, 2019. For this purpose, each time a new small EQ takes place we calculate the κ_1 values corresponding to the events that occurred within all the possible subareas that include this EQ (Sarlis et al., 2008). This procedure leads to an ensemble of κ_1 values from which we can calculate the probability Prob(κ_1) of κ_1 to lie within $\kappa_1 \pm 0.025$. Figures 4(a), (b), (c), and (d) depict the histograms of Prob(κ_1) obtained after the occurrence of each small EQ with magnitude greater than or equal to 2.3, 2.4, 2.6, and 2.7, respectively. We observe that upon the occurrence of a M3.4 EQ at 22:41 UTC on July 2, 2019 at 35.050^{o}N 118.936^{o}W all the four distributions Prob(κ_1) exhibit a maximum at $\kappa_1 = 0.070$. This behavior has been assured to occur a few days up to one week or so before the strong EQ occurrence (Sarlis et al., 2008; Varotsos et al., 2010, 2011c, 2015b, 2017a; Sarlis and Skordas, 2018). Actually, two days later the (first) M6.4 Ridgecrest EQ occurred that was followed by the M7.1 Ridgecrest EQ on July 6, 2019.

5 Discussion

We first comment on the behavior of the order parameter fluctuations depicted in Figs.2 and 3: As already mentioned the minima of β_W for W =300, 350, 400, and 450 that are observed on June 5, 2019, are global minima for the whole period of our study. Varotsos et al. (2011a); Sarlis et al. (2013); Varotsos et al. (2014); Sarlis et al. (2019a) have presented case studies in California, Greece, Japan, and Mexico, in which the variability minima before the strongest EQs in each of these regional studies were the deepest one. In our case, however, although the 2010 El Mayor-Cucapah M7.3 EQ is the strongest EQ in our study period (see Fig.2) the aforementioned deepest minima are observed before the 2019 M7.1 Ridgecrest EQ. This can be understood on the basis of the fact that the Ridgecrest EQ epicenter lies closer to the center of our study area, depicted by the green line in Fig.1, than the one of the 2010 El Mayor-Cucapah EQ that lies in the southern east bottom margin. Thus, when looking for the global variability minimum one should also take into account the epicenter locations of the strongest EQs in the area. Returning now to the behavior of the order parameter fluctations a few months before the 2019 M7.1 Ridgecrest EQ, an inspection of Fig.3(a) reveals that all β_W exhibited an initial decrease after approximately February 10, 2019, and gradually approached their minimum values during the period May, 29 to June, 5, 2019. Figure 3(b) reveals that when these minima are reached the corresponding DFA exponent a_{300} values were above $a = 0.5$ pointing to the presence of long-range correlations. In order to assert the presence of long-range correlations during the formation of β_{min}, we used surrogate data by randomly shuffling the EQ magnitudes that led to the DFA behavior depicted in Fig.3(a) from 1 February 2019 until 5 June 2019, i.e., when β_W's started to decrease. We produced 10^3 surrogate time-series, performed DFA and found that the distribution of the average value of a_{300} during this period follows a Gaussian distribution with mean value 0.523544 and standard deviation 0.0374564. On the other hand, the DFA values depicted in Fig.3(a) during the same period resulted in an average value $\langle a_{300} \rangle$=0.587173, that leads to a z-score ≈ 1.7, which corresponds to a probability Prob($z > 1.7$) = 4.46 % to be obtained by chance from the surrogate data. Thus, the observed DFA values are highly unlikely to come from randomly distributed EQ magnitudes since they exceed the corresponding 95% confidence interval.

We now comment on the DFA exponent a_{300} behavior. As already mentioned, it has been found (Lennartz et al., 2008; Sarlis et al., 2010a) that during the regimes of stationary seismic activity a values around 0.6 are observed. This is reflected by the a_{300}-values shown in Fig.2(c) that exhibit an average behavior which is well above 0.5 and close to 0.6. Additionally, Varotsos et al. (2014); Sarlis et al. (2019b,a) have discussed the importance of the change of temporal correlations between EQ magnitudes during the period before a strong EQ occurrence: For example, upon the observation of β_{min} before the 2011 M9 Tohoku EQ the a value was well above 0.5 (see Table 4 of Varotsos et al., 2014) while later it fall below 0.5 pointing to anticorrelation(cf. a similar behavior was observed before the 2017 M8.2 Chiapas EQ, see Fig.3 of Sarlis et al., 2019a). In a similar fashion to these observations, Fig.3(c) reveals that after the aforementioned long-range correlated behavior and before the 2019 M7.1 Ridgecrest the a_{300} values of the EQ magnitude time-series returned to random behavior being close (or even smaller) than 0.5 (see the rightmost part of this panel).

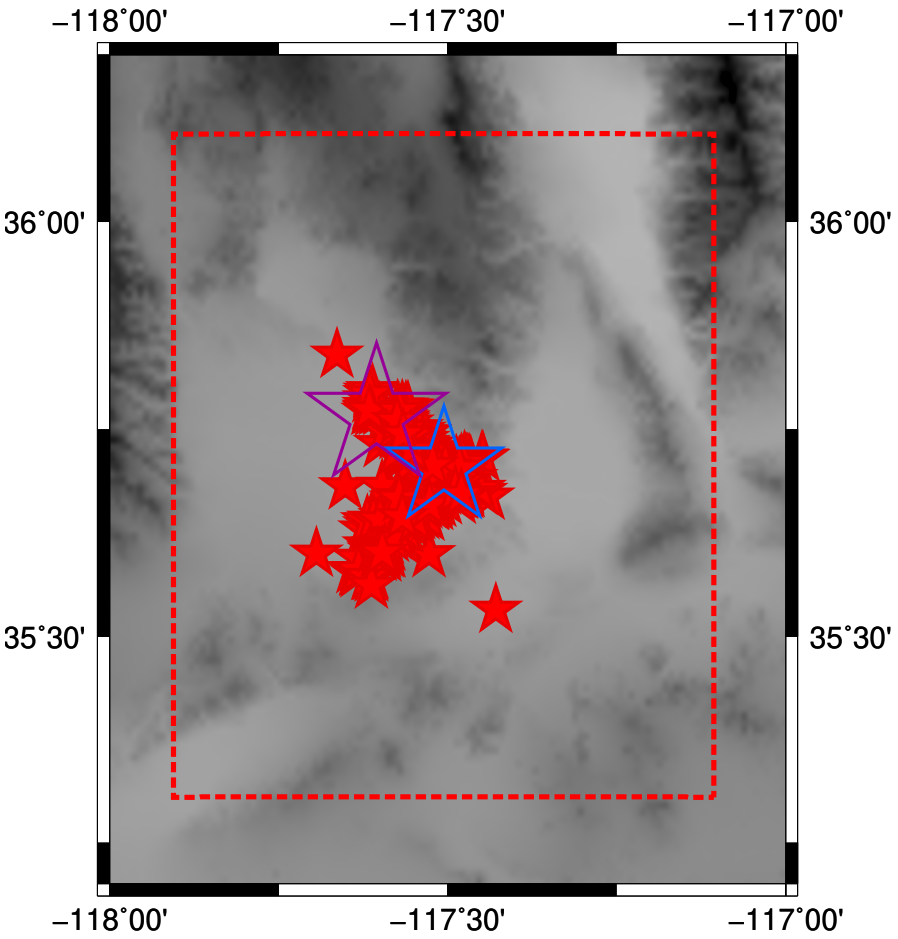

Fig. 5 (color online) The small EQs with $M \geq 2.0$ that occurred after the M6.4 EQ on July 4, 2019 (blue star), and before the M7.1 Ridgecrest EQ (magenta star) within a $0.4^o \times 0.4^o$ rectangle (red dashed lines) centered at the first event (for the rules of selecting the size of the area see Christopoulos and Sarlis (2017)).

Finally, we comment on the possible application of a recent method(Christopoulos and Sarlis, 2017) based on the coherent noise model (Newman and Sneppen, 1996; Newman, 1996; Sneppen and Newman, 1997) for the estimation of the time of occurrence of the strongest aftershock. According to this method(Christopoulos and Sarlis, 2017) upon the occurrence of a strong EQ of magnitude M_{ms}, the seismicity in the aftershock area, which is estimated on the basis of a rectangle of linear size that scales as $10^{0.5\mathrm{M}_{ms}}$ centered at the epicenter of the strong EQ, is studied and a time-series labeled e_k is constructed as follows: The first element e_1 of the time series e_k is equal to one and corresponds to the first aftershock after the mainshock. Each subsequent e_k is obtained as follows: If the magnitude of the aftershock is smaller than the previous $k-1$-th aftershock then we increase the value e_{k-1} by one to obtain e_k (e.g. if we have a previous aftershock of magnitude M4.3 and the e_{k-1} corresponds to 4 and the current aftershock has magnitude

M3.2 the e_k is equal to 4+1=5). If the aftershock magnitude is higher than that of the previous aftershock, we successively examine all past aftershocks starting from the present until we reach one that has higher magnitude. Let us assume that this is the m-th aftershock, then $e_k = e_m + 1$. If there is no such aftershock, we set e_k=1. The strongest aftershocks are expected to occur when e_k is smaller than or equal to a threshold e_t; for example in Southern California the value $e_t = 5$ has been suggested(see Fig.13(a) of Christopoulos and Sarlis, 2017). In our case, Fig. 5 depicts the aftershock area that corresponds to the M6.4 Ridgecrest EQ on July 4, 2019, together with the aftershocks that occurred there until the M7.1 Ridgecrest EQ on July 6, 2019. The construction of the time-series e_k in this case, reveals that $e_k = 2$ almost three minutes before the M7.1 Ridgecrest EQ due to the occurrence of the two strong aftershocks, which can be seen in Fig.3(c), i.e., a M5.36 EQ at 07:53 UTC on July 5, 2019, and the M4.97 at 03:16 UTC on July 6, 2019. This result combined with the aforementioned fact that seismicity has reached criticality at 22:41 UTC on July 2, 2019 (see Sect. 4) lead us to conclude that the occurrence time of the M7.1 Ridgecrest EQ might have been anticipated well in advance, while its epicenter could have been determined on the basis of the M6.4 Ridgecrest EQ on July 4, 2019 (see Fig.5).

6 Conclusions

The following three important features have been revealed from the study of the seismicity in Southern California before the 2017 M7.1 Ridgecrest EQ that occurred on July 6, 2019:

1. On June 5, 2019, the fluctuations of the order parameter of seismicity exhibited a minimum β_{min}.
2. The temporal correlations between EQ magnitudes as identified by DFA showed that the initial long-range correlations ($a_{300} \approx 0.6$) on June 5 were destroyed before the M7.1 EQ occurrence since a behavior close random ($a = 0.5$)was later observed.
3. The natural time analysis of seismicity after the occurrence of β_{min} reveals that criticality has been reached almost three days before the M7.1 EQ occurrence, i.e., at 22:41 UTC on July 2, 2019.

The present results when considered together with those obtained from the recent strong EQs in Japan and Mexico may help us understand the preseismic processes and forecast their occurrence.

Conflict of interest

The authors declare that they have no conflict of interest.

References

Ashkenazy Y, Hausdorff JM, Ivanov PC, Stanley HE (2002) A stochastic model of human gait dynamics. Physica A 316:662–670, DOI 10.1016/S0378-4371(02)01453-X

Bashan A, Bartsch R, Kantelhardt JW, Havlin S (2008) Comparison of detrending methods for fluctuation analysis. Physica A 387:5080 – 5090, DOI 10.1016/j.physa.2008.04.023

Bird P (2003) An updated digital model of plate boundaries. Geochemistry, Geophysics, Geosystems 4:1027, DOI 10.1029/2001GC000252

Buldyrev SV, Goldberger AL, Havlin S, Mantegna RN, Matsa ME, Peng CK, Simons M, Stanley HE (1995) Long-range correlation properties of coding and noncoding dna sequences: Genbank analysis. Phys Rev E 51:5084–5091

Bunde A, Havlin S, Kantelhardt JW, Penzel T, Peter JH, Voigt K (2000) Correlated and uncorrelated regions in heart-rate fluctuations during sleep. Phys Rev Lett 85:3736–3739, DOI 10.1103/physrevlett.85.3736

Carlson JM, Langer JS, Shaw BE (1994) Dynamics of earthquake faults. Rev Mod Phys 66:657–670, DOI 10.1103/RevModPhys.66.657

Carpena P, Bernaola-Galván P, Ivanov PC, Stanley HE (2002) Metal-insulator transition in chains with correlated disorder. Nature (London) 418:955

Chen Z, Ivanov PC, Hu K, Stanley HE (2002) Effect of nonstationarities on detrended fluctuation analysis. Phys Rev E 65:041107

Chen Z, Hu K, Carpena P, Bernaola-Galvan P, Stanley HE, Ivanov PC (2005) Effect of nonlinear filters on detrended fluctuation analysis. Phys Rev E 71:011104

Christopoulos SRG, Sarlis NV (2017) An Application of the Coherent Noise Model for the Prediction of Aftershock Magnitude Time Series. Complexity 2017:6853892, DOI 10.1155/2017/6853892

Goldberger AL, Amaral LAN, Glass L, Hausdorff JM, Ivanov PC, Mark RG, Mictus JE, Moody GB, Peng CK, Stanley HE (2000) Physiobank, physiotoolkit, and physionet - components of a new research resource for complex physiologic signals. Circulation 101:E215 (see also `www.physionet.org`), DOI 10.1161/01.CIR.101.23.e215

Gutenberg B, Richter CF (1956) Magnitude and energy of earthquakes. Ann Geophys 9:1–15

Han P, Hattori K, Xu G, Ashida R, Chen CH, Febriani F, Yamaguchi H (2015) Further investigations of geomagnetic diurnal variations associated with the 2011 off the Pacific coast of Tohoku earthquake (Mw 9.0). J Asian Earth Sci 114:321 – 326

Han P, Hattori K, Huang Q, Hirooka S, Yoshino C (2016) Spatiotemporal characteristics of the geomagnetic diurnal variation anomalies prior to the 2011 Tohoku earthquake (Mw 9.0) and the possible coupling of multiple pre-earthquake phenomena. J Asian Earth Sci 129:13 – 21

Hauksson E, Yang W, Shearer PM (2012) Waveform Relocated Earthquake Catalog for Southern California (1981 to June 2011). Bull Seismol Soc Am 102:2239–2244, DOI 10.1785/0120120010

Holliday JR, Rundle JB, Turcotte DL, Klein W, Tiampo KF, Donnellan A (2006) Space-time clustering and correlations of major earthquakes. Phys Rev Lett 97:238501, DOI 10.1103/PhysRevLett.97.238501

Hu K, Ivanov PC, Chen Z, Carpena P, Stanley HE (2001) Effect of trends on detrended fluctuation analysis. Phys Rev E 64:011114, DOI 10.1103/physreve.64.011114

Hu K, Ivanov PC, Chen Z, Hilton MF, Stanley HE, Shea SA (2004) Non-random fluctuations and multi-scale dynamics regulation of human activity. Physica A 337:307

Huang Q (2008) Seismicity changes prior to the Ms8.0 Wenchuan earthquake in Sichuan, China. Geophys Res Lett 35:L23308, DOI 10.1029/2008GL036270

Huang Q (2011) Retrospective investigation of geophysical data possibly associated with the Ms8.0 Wenchuan earthquake in Sichuan, China . Journal of Asian Earth Sciences 41:421 – 427, DOI 10.1016/j.jseaes.2010.05.014

Huang Q, Ding X (2012) Spatiotemporal variations of seismic quiescence prior to the 2011 M 9.0 Tohoku earthquake revealed by an improved region-time-length algorithm. Bull Seismol Soc Am 102:1878–1883, DOI 10.1785/0120110343

Ivanov PC, Nunes Amaral LA, Goldberger AL, Stanley HE (1998) Stochastic feedback and the regulation of biological rhythms. Europhys Lett 43:363

Ivanova K, Ausloos M (1999) Application of the detrended fluctuation analysis (DFA) method for describing cloud breaking. Physica A 274:349–354, DOI 10.1016/s0378-4371(99)00312-x

Kanamori H (1978) Quantification of earthquakes. Nature 271:411–414, DOI 10.1038/271411a0

Kanamori H, Brodsky EE (2001) The Physics of Earthquakes. Physics Today 54(6):34–40, DOI 10.1063/1.1387590

Kantelhardt JW, Koscielny-Bunde E, Rego HHA, Havlin S, Bunde A (2001) Detecting long-range correlations with detrended fluctuation analysis. Physica A 295:441 – 454, DOI 10.1016/s0378-4371(01)00144-3

Koscielny-Bunde E, Bunde A, Havlin S, Roman HE, Goldreich Y, Schellnhuber HJ (1998) Indication of a universal persistence law governing atmospheric variability. Phys Rev Lett 81:729

Lennartz S, Livina VN, Bunde A, Havlin S (2008) Long-term memory in earthquakes and the distribution of interoccurrence times. EPL (Europhysics Letters) 81:69001, DOI 10.1209/0295-5075/81/69001

Lennartz S, Bunde A, Turcotte DL (2011) Modelling seismic catalogues by cascade models: Do we need long-term magnitude correlations? Geophys J Int 184:1214–1222, DOI 10.1111/j.1365-246X.2010.04902.x

Lippiello E, de Arcangelis L, Godano C (2008) Influence of time and space correlations on earthquake magnitude. Phys Rev Lett 100:038501, DOI 10.1103/PhysRevLett.100.038501

Luginbuhl M, Rundle JB, Turcotte DL (2018) Natural Time and Nowcasting Earthquakes: Are Large Global Earthquakes Temporally Clustered? Pure and Applied Geophysics 175:661–670, DOI 10.1007/s00024-018-1778-0

Newman MEJ (1996) Self-organized criticality, evolution and the fossil extinction record. Proc R Soc London B 263:1605–1610, DOI 10.1098/rspb.1996.0235

Newman MEJ, Sneppen K (1996) Avalanches, scaling, and coherent noise. Phys Rev E 54:6226–6231, DOI 10.1103/physreve.54.6226

Peng CK, Buldyrev SV, Goldberger AL, Havlin S, Simons M, Stanley HE (1993) Finite-size effects on long-range correlations: Implications for analyzing DNA sequences. Phys Rev E 47:3730–3733, DOI 10.1103/physreve.47.3730

Peng CK, Buldyrev SV, Havlin S, Simons M, Stanley HE, Goldberger AL (1994) Mosaic organization of DNA nucleotides. Phys Rev E 49:1685–1689, DOI 10.1103/physreve.49.1685

Peng CK, Buldyrev SV, Goldberger AL, Havlin S, Mantegna RN, Simons M, Stanley HE (1995a) Statistical properties of dna sequences. Physica A 221:180–192, DOI 10.1016/0378-4371(95)00247-5

Peng CK, Havlin S, Stanley HE, Goldberger AL (1995b) Quantification of scaling exponents and crossover phenomena in nonstationary heartbeat time series. Chaos 5:82–87, DOI 10.1063/1.166141

Rundle JB, Turcotte DL, Klein W (2000) (eds.) GeoComplexity and the Physics of Earthquakes. AGU, Washington, DC

Rundle JB, Holliday JR, Graves WR, Turcotte DL, Tiampo KF, Klein W (2012) Probabilities for large events in driven threshold systems. Phys Rev E 86:021106

Rundle JB, Turcotte DL, Donnellan A, Grant Ludwig L, Luginbuhl M, Gong G (2016) Nowcasting earthquakes. Earth and Space Science 3:480–486, DOI 10.1002/2016EA000185

Rundle JB, Giguere A, Turcotte DL, Crutchfield JP, Donnellan A (2019) Global Seismic Nowcasting With Shannon Information Entropy. Earth and Space Science 6(1):191–197, DOI 10.1029/2018EA000464

Sarlis N, Varotsos P (2002) Magnetic field near the outcrop of an almost horizontal conductive sheet. J Geodynamics 33:463–476

Sarlis N, Skordas E, Varotsos P (2011) Similarity of fluctuations in systems exhibiting Self-Organized Criticality. EPL (Europhysics Letters) 96:28006, DOI 10.1209/0295-5075/96/28006

Sarlis NV (2013) On the recent seismic activity in North-Eastern Aegean Sea including the M_w 5.8 earthquake on 8 January 2013. Proc Jpn Acad Ser B Phys Biol Sci 89:438–445, DOI 10.2183/pjab.89.438

Sarlis NV (2017) Entropy in Natural Time and the Associated Complexity Measures. Entropy 19(4), DOI 10.3390/e19040177

Sarlis NV, Skordas ES (2018) Study in Natural Time of Geoelectric Field and Seismicity Changes Preceding the Mw6.8 Earthquake on 25 October 2018 in Greece. Entropy 20:882, DOI 10.3390/e20110882

Sarlis NV, Skordas ES, Lazaridou MS, Varotsos PA (2008) Investigation of seismicity after the initiation of a Seismic Electric Signal activity until the main shock. Proc Jpn Acad Ser B Phys Biol Sci 84:331–343, DOI 10.2183/pjab.84.331

Sarlis NV, Skordas ES, Varotsos PA (2010a) Nonextensivity and natural time: The case of seismicity. Phys Rev E 82:021110, DOI 10.1103/physreve.82.021110

Sarlis NV, Skordas ES, Varotsos PA (2010b) Order parameter fluctuations of seismicity in natural time before and after mainshocks. EPL 91:59001, DOI 10.1209/0295-5075/91/59001

Sarlis NV, Skordas ES, Varotsos PA, Nagao T, Kamogawa M, Tanaka H, Uyeda S (2013) Minimum of the order parameter fluctuations of seismicity before major earthquakes in Japan. Proc Natl Acad Sci USA 110:13734–13738, DOI 10.1073/pnas.1312740110

Sarlis NV, Skordas ES, Varotsos PA, Nagao T, Kamogawa M, Uyeda S (2015) Spatiotemporal variations of seismicity before major earthquakes in the Japanese area and their relation with the epicentral locations. Proc Natl Acad Sci USA 112:986–989, DOI 10.1073/pnas.1422893112

Sarlis NV, Skordas ES, Mintzelas A, Papadopoulou KA (2018a) Micro-scale, mid-scale, and macro-scale in global seismicity identified by empirical mode decomposition and their multifractal characteristics. Scientific Reports 8:9206, DOI 10.1038/s41598-018-27567-y

Sarlis NV, Skordas ES, Varotsos PA (2018b) Chapter 7 - natural time analysis of seismic time series. In: Chelidze T, Vallianatos F, Telesca L (eds) Complexity of Seismic Time Series, Elsevier, pp 199 – 235, DOI 10.1016/B978-0-12-813138-

1.00007-9
Sarlis NV, Varotsos PA, Skordas ES, Zlotnicki J, Nagao T, Rybin A, Lazaridou-Varotsos MS, Papadopoulou K (2018c) Seismic electric signals in seismic prone areas. Earthquake Science 31:44–51, DOI 10.29382/eqs-2018-0005-5
Sarlis NV, Skordas ES, Varotsos PA, Ramrez-Rojas A, Flores-Mrquez EL (2019a) Identifying the occurrence time of the deadly mexico m8.2 earthquake on 7 september 2017. Entropy 21(3), DOI 10.3390/e21030301, URL https://www.mdpi.com/1099-4300/21/3/301
Sarlis NV, Skordas ES, Varotsos PA, Ramrez-Rojas A, Flores-Mrquez EL (2019b) Investigation of the temporal correlations between earthquake magnitudes before the Mexico M8.2 earthquake on 7 September 2017. Physica A 517:475 – 483, DOI 10.1016/j.physa.2018.11.041
Skordas E, Sarlis N (2014) On the anomalous changes of seismicity and geomagnetic field prior to the 2011 9.0 Tohoku earthquake. J Asian Earth Sci 80:161 – 164, DOI 10.1016/j.jseaes.2013.11.008
Sneppen K, Newman M (1997) Coherent noise, scale invariance and intermittency in large systems. Physica D 110:209 – 222, DOI 10.1016/s0167-2789(97)00128-0
Stratonovich RL (1981) Topics in the theory of random noise Vol. I. Gordon and Breach, New York
Talkner P, Weber RO (2000) Power spectrum and detrended fluctuation analysis: Application to daily temperatures. Phys Rev E 62:150–160, DOI 10.1103/physreve.62.150
Tanaka HK, Varotsos PA, Sarlis NV, Skordas ES (2004) A plausible universal behaviour of earthquakes in the natural time-domain. Proc Jpn Acad Ser B Phys Biol Sci 80:283–289, DOI 10.2183/pjab.80.283
Taqqu MS, Teverovsky V, Willinger W (1995) Estimators for long-range dependence: An empirical study. Fractals 3:785–798
Telesca L, Lovallo M (2009) Non-uniform scaling features in central Italy seismicity: A non-linear approach in investigating seismic patterns and detection of possible earthquake precursors. Geophys Res Lett 36:L01308, DOI 10.1029/2008GL036247
Telesca L, Lapenna V, Macchiato M (2003) Spatial variability of the time-correlated behaviour in Italian seismicity. Earth and Planetary Science Letters 212:279 – 290, DOI 10.1016/S0012-821X(03)00286-3
Turcotte DL (1997) Fractals and Chaos in Geology and Geophysics, 2nd edn. Cambridge University Press, Cambridge, DOI 10.1017/CBO9781139174695
Utsu T, Ogata Y, S R, Matsu'ura (1995) The Centenary of the Omori Formula for a Decay Law of Aftershock Activity. Journal of Physics of the Earth 43(1):1–33, DOI 10.4294/jpe1952.43.1
Uyeda S, Hayakawa M, Nagao T, Molchanov O, Hattori K, Orihara Y, Gotoh K, Akinaga Y, Tanaka H (2002) Electric and magnetic phenomena observed before the volcano-seismic activity in 2000 in the Izu Island Region, Japan. Proc Natl Acad Sci USA 99:7352–7355, DOI 10.1073/pnas.072208499
Uyeda S, Kamogawa M, Tanaka H (2009) Analysis of electrical activity and seismicity in the natural time domain for the volcanic-seismic swarm activity in 2000 in the Izu Island region, Japan. J Geophys Res 114:B02310, DOI 10.1029/2007JB005332
Varotsos CA, Lovejoy S, Sarlis NV, Tzanis CG, Efstathiou MN (2015a) On the scaling of the solar incident flux. Atmospheric Chemistry and Physics

15(13):7301–7306, DOI 10.5194/acp-15-7301-2015
Varotsos P (2005) The Physics of Seismic Electric Signals. TERRAPUB, Tokyo
Varotsos P, Lazaridou M (1991) Latest aspects of earthquake prediction in Greece based on Seismic Electric Signals. Tectonophysics 188:321–347, DOI 10.1016/0040-1951(91)90462-2
Varotsos P, Alexopoulos K, Lazaridou M (1993) Latest aspects of earthquake prediction in Greece based on Seismic Electric Signals,II. Tectonophysics 224:1 – 37, DOI 10.1016/0040-1951(93)90055-O
Varotsos P, Sarlis N, Skordas E (2011a) Scale-specific order parameter fluctuations of seismicity in natural time before mainshocks. EPL 96:59002, DOI 10.1209/0295-5075/96/59002
Varotsos P, Sarlis NV, Skordas ES, Uyeda S, Kamogawa M (2011b) Natural time analysis of critical phenomena. Proc Natl Acad Sci USA 108:11361–11364, DOI 10.1073/pnas.1108138108
Varotsos P, Sarlis N, Skordas E (2012) Scale-specific order parameter fluctuations of seismicity before mainshocks: Natural time and detrended fluctuation analysis. EPL 99:59001, DOI 10.1209/0295-5075/99/59001
Varotsos PA, Sarlis NV, Skordas ES (2001) Spatio-temporal complexity aspects on the interrelation between seismic electric signals and seismicity. Practica of Athens Academy 76:294–321, http://physlab.phys.uoa.gr/org/pdf/p3.pdf
Varotsos PA, Sarlis NV, Skordas ES (2002a) Long-range correlations in the electric signals that precede rupture. Phys Rev E 66:011902, DOI 10.1103/physreve.66.011902
Varotsos PA, Sarlis NV, Skordas ES (2002b) Seismic electric signals and seismicity: On a tentative interrelation between their spectral content. Acta Geophysica Polonica 50:337–354
Varotsos PA, Sarlis NV, Skordas ES (2003a) Attempt to distinguish electric signals of a dichotomous nature. Phys Rev E 68:031106, DOI 10.1103/PhysRevE.68.031106
Varotsos PA, Sarlis NV, Skordas ES (2003b) Long-range correlations in the electric signals the precede rupture: Further investigations. Phys Rev E 67:021109, DOI 10.1103/PhysRevE.67.021109
Varotsos PA, Sarlis NV, Tanaka HK, Skordas ES (2005) Similarity of fluctuations in correlated systems: The case of seismicity. Phys Rev E 72:041103, DOI 10.1103/physreve.72.041103
Varotsos PA, Sarlis NV, Skordas ES, Lazaridou MS (2008) Fluctuations, under time reversal, of the natural time and the entropy distinguish similar looking electric signals of different dynamics. J Appl Phys 103:014906, DOI 10.1063/1.2827363
Varotsos PA, Sarlis NV, Skordas ES, Uyeda S, Kamogawa M (2010) Natural time analysis of critical phenomena. the case of seismicity. EPL 92:29002, DOI 10.1209/0295-5075/92/29002
Varotsos PA, Sarlis NV, Skordas ES (2011c) Natural Time Analysis: The new view of time. Precursory Seismic Electric Signals, Earthquakes and other Complex Time-Series. Springer-Verlag, Berlin Heidelberg, DOI 10.1007/978-3-642-16449-1
Varotsos PA, Sarlis NV, Skordas ES, Lazaridou MS (2013) Seismic Electric Signals: An additional fact showing their physical interconnection with seismicity. Tectonophysics 589:116–125, DOI 10.1016/j.tecto.2012.12.020

Varotsos PA, Sarlis NV, Skordas ES (2014) Study of the temporal correlations in the magnitude time series before major earthquakes in Japan. J Geophys Res: Space Physics 119:9192–9206, DOI 10.1002/2014JA020580

Varotsos PA, Sarlis NV, Skordas ES, Christopoulos SRG, Lazaridou-Varotsos MS (2015b) Identifying the occurrence time of an impending mainshock: a very recent case. Earthquake Science 28(3):215, DOI 10.1007/s11589-015-0122-3

Varotsos PA, Sarlis NV, Skordas ES (2017a) Identifying the occurrence time of an impending major earthquake: a review. Earthquake Science 30(4):209–218, DOI 10.1007/s11589-017-0182-7

Varotsos PA, Sarlis NV, Skordas ES, Lazaridou-Varotsos MS (2017b) $M_W 9$ Tohoku earthquake in 2011 in Japan: precursors uncovered by natural time analysis. Earthquake Science pp 1–9, DOI 10.1007/s11589-017-0189-0

Varotsos PA, Sarlis NV, Skordas ES (2019) Phenomena preceding major earthquakes interconnected through a physical model. Annales Geophysicae 37(3):315–324, DOI 10.5194/angeo-37-315-2019, URL https://www.ann-geophys.net/37/315/2019/

Xu G, Han P, Huang Q, Hattori K, Febriani F, Yamaguchi H (2013) Anomalous behaviors of geomagnetic diurnal variations prior to the 2011 off the Pacific coast of Tohoku earthquake (Mw9.0). J Asian Earth Sci 77:59 – 65

Xu L, Ivanov PC, Hu K, Chen Z, Carbone A, Stanley HE (2005) Quantifying signals with power-law correlations: A comparative study of detrended fluctuation analysis and detrended moving average techniques. Phys Rev E 71:051101, DOI 10.1103/physreve.71.051101